Theory of Direct-Interaction Inelastic Scattering*

NORMAN K. GLENDENNING
Lawrence Radiation Laboratory, University of California, Berkeley, California
(Received January 12, 1959)

A model is proposed for the description of direct-interaction inelastic scattering in which resolved final states of the target nucleus are observed. This model is expected to be useful in deducing the spins and parities of the excited states of nuclei.

I. INTRODUCTION

SINCE the development of the theory of deuteron stripping by Butler and others[1–3] the analysis of the angular distributions in these reactions which leave the residual nucleus in some definite quantum state has provided an important means of investigating the properties of low-lying states in nuclei. The usefulness of the stripping reaction in this respect is probably due to two important features of the process: it is a direct interaction, and it occurs near the nuclear surface. Of course experimental conditions can be found in which compound-nucleus contributions are appreciable, but these should be avoided in seeking data to yield information on the spins and parities of the states of the residual nucleus.

Another process which one might expect to be characterized by the above features is the inelastic scattering of nucleons by complex nuclei, in which the incident particle transfers energy and angular momentum to a single bound nucleon leaving the target in an excited state. This process is usually referred to as direct-interaction scattering, and has been treated theoretically by a number of authors. One uses the shell-model picture of the nucleus, with the direct interaction acting between the incident particle and a nucleon in the outer shell. The first-order processes of course involves the change in the quantum numbers of only one bound nucleon.

The first theoretical treatment of direct-interaction inelastic scattering was given by Austern, Butler, and McManus.[4] They assumed a zero-range surface interaction with spinless particles, and neglect the elastic scattering and partial absorption of the incident particle before and after the direct interaction. Their theory has met with moderate success in predicting angular distributions, especially in fitting peaks at forward angles, but fails conspicuously in other cases. An example of its failure is illustrated in Fig. 10 in which a comparison is made with the experimental data on C^{12}. The theoretical cross section predicted by Austern *et al.* does not, in general, give sufficiently reliable results to yield information on the spins and parities of the nuclear states.

The most complete treatment of the direct-interaction process is given by Levinson and Banerjee.[5] They take account of the elastic scattering of the free nucleon before and after the direct interaction by using waves distorted by a complex potential. Moreover, the direct interaction is allowed to occur throughout the entire nuclear volume. The theory agrees quite well with the carbon data over a wide range of energies. Unfortunately the numerical calculation is very lengthy, requiring considerable high-speed computer time. Since, as a tool for the nuclear spectroscopist, the theory is required only to be good enough to distinguish between different assumptions about the nuclear states involved, it seemed worth while to attempt to formulate a simpler model that would still satisfy the above requirement. That is the object of this work.

In the treatment of direct interactions presented here, a surface interaction is used, and the free particle is allowed to interact with the whole nucleus before and after the direct inelastic event. It is shown how all the integrations can be performed explicitly, thus reducing the calculation time required in an attempt to analyze experimental data by means of the model.

II. COMPETITION BETWEEN DIRECT REACTIONS AND COMPOUND-NUCLEUS FORMATION

Weisskopf concludes from the experimental data that nuclear reactions with neutrons involve the formation of a compound nucleus with an 80 to 90% probability.[6] Nevertheless it is quite possible that the low-lying states of the target nucleus may be excited almost exclusively by the direct-interaction mechanism, for bombarding energies greater than a few Mev. This follows from a rather important difference between the two modes of excitation. In inelastic scattering through a compound-nucleus channel, the reaction proceeds through the formation and independent decay of a compound state, which separates the initial and final states of the target nucleus. For incident bombarding energies of a few Mev, a large number of states in the residual nucleus can be excited with comparable probability, so that the cross section for excitation of a

* Summary of a thesis presented to the Department of Physics, Indiana University, 1958.
[1] S. T. Butler, Proc. Roy. Soc. (London) **A208**, 559 (1951).
[2] Bhatia, Huang, Huby, and Newns, Phil. Mag. **43**, 485 (1952).
[3] P. B. Daitch and J. B. French, Phys. Rev. **87**, 900 (1952).
[4] Austern, Butler, and McManus, Phys. Rev. **92**, 350 (1953).
[5] C. A. Levinson and M. K. Banerjee, Ann. Phys. **2**, 471 (1957); **2**, 499 (1957); **3**, 67 (1958).
[6] V. F. Weisskopf, Revs. Modern Phys. **29**, 174 (1957).

given nuclear level may be very small. However, in scattering by direct interaction the two-body force between incident and bound particles is regarded as a perturbation causing transitions of the system from its initial state. Therefore the cross section depends on the matrix element of the direct interaction taken between initial and final states of the entire system, and accordingly is very sensitive to the overlap of the system states. Moreover, the lowest-order process involves a transition between nuclear states that differ in the quantum numbers of only one nucleon. Accordingly, the low-lying levels in the residual nucleus are those most strongly excited by the direct interaction, and amongst these, certain levels are more strongly excited than others because of selection rules and overlap of the shell-model states involved.

Thus in formation of a compound nucleus by neutrons of more than a few Mev, the number of competing states to which the compound nucleus can decay is so large that the cross section for excitation of any given one of them is small. However, for direct reactions, which strongly favor the excitation of only a few low-lying states, there are few "competing" states even at high incident energies. For these reasons the direct-interaction process is expected to dominate the compound-nucleus process in excitation of the low-lying levels of the final nucleus, for incident energies greater than a few Mev. These remarks are valid, of course, for protons as well.

The most striking evidence that the compound-nucleus contribution to the excitation of low-lying levels is often small is found in the strong forward-hemisphere scattering of nucleon groups leaving the nucleus in a particular quantum state.[7–10] The compound-nucleus theory predicts an angular distribution that is symmetric about 90° or else isotropic.[11] Moreover, the magnitudes of the observed cross sections are frequently much larger than can be explained by the compound-nucleus theory.

III. SURFACE EFFECT IN DIRECT REACTIONS

An attempt is made here to make plausible the assumption of a surface interaction for the direct-interaction scattering mechanism.

The energy dependence of the real and imaginary parts of the optical-model potential, as found by Melkanoff *et al.*,[12] imply that the mean free path of protons in nuclear matter follows the rule

$$\Lambda = K^{-1} \gtrsim r_0, \quad \text{for} \quad E < 10 \text{ Mev}, \qquad \lesssim r_0, \quad \text{for} \quad E > 10 \text{ Mev}, \tag{1}$$

where r_0 is a typical nuclear radius, say $6\text{–}8\times10^{-13}$ cm, E is the incident energy, and K is the absorption coefficient, equal to the imaginary part of the complex propagation number inside the nucleus. Only for energies less than a few Mev or greater than, say, 100 Mev does the nucleus become rather transparent. One may expect that once an incident nucleon of intermediate energy penetrates to a depth of a mean free length or more into the nucleus, the probability that a compound state will be formed is very large. This suggests that the direct interactions take place before the incident particle has penetrated to within a mean free length into the nucleus, and for incident energies $E \gtrsim 10$ Mev this means that they take place near the nuclear surface. Using somewhat different language, one can say that, since the incident nucleon should be regarded as moving in the presence of the complex optical potential, its wave function will be damped exponentially as the particle enters the nucleus.

Bjorklund *et al.*[13,14] take a rather different view of the absorption of nucleons by complex nuclei. They have proposed a surface absorption model which has been quite successful in predicting elastic scattering and polarizations of scattered neutrons. However, whichever view is more correct, both imply that the direct process is concentrated near the nuclear surface.

The bound particles themselves that become excited by the direct interaction are usually those whose probability density tends to be concentrated near the nuclear surface, for a nucleon entering the nucleus cannot interact with one of the more tightly bound nucleons unless both particles scatter into unoccupied states. This requires a large energy transfer, and in Sec. II it was argued that this is less probable than a small energy transfer. Accordingly the bound nucleons that participate most freely in direct reactions are the loosely bound nucleons. Such nucleons generally are concentrated near the nuclear surface.

In addition to these arguments, the results of some calculations are presented in Sec. V which tend to justify the use of a surface interaction.

IV. CALCULATION OF DIRECT-INTERACTION INELASTIC CROSS SECTION

1. Brief Description of the Calculation

The success of the shell model in describing the low-energy properties of nuclei[15–20] sugests that direct-interaction scattering may well be discussed in the

[7] E. H. Rhoderick, Proc. Roy. Soc. (London) **A201**, 348 (1950).
[8] H. McManus and W. T. Sharp, Phys. Rev. **87**, 188 (1952).
[9] R. M. Eisberg and G. Igo, Phys. Rev. **93**, 1039 (1954).
[10] Shrank, Gugelot, and Dayton, Phys. Rev. **96**, 1156 (1954).
[11] W. Hauser and H. Feshbach, Phys. Rev. **87**, 366 (1952).
[12] Melkanoff, Moszkowski, Nodvick, and Saxon, Phys. Rev. **101**, 507 (1956).
[13] Bjorklund, Fernbach, and Sherman, Phys. Rev. **101**, 1832L (1956).
[14] F. Bjorklund and S. Fernbach, Phys. Rev. **109**, 1295 (1958).
[15] M. G. Mayer and J. H. D. Jensen, *Elementary Theory of Nuclear Shell Structure* (John Wiley and Sons, Inc., New York, 1955).
[16] M. H. L. Pryce, Proc. Phys. Soc. (London) **A65**, 773 (1952).
[17] K. W. Ford and C. Levinson, Phys. Rev. **99**, 792 (1955); **100**, 1 (1955); **100**, 13 (1955).
[18] D. Kurath, Phys. Rev. **101**, 216 (1956).
[19] S. Goldstein and I. Talmi, Phys. Rev. **105**, 995 (1957).
[20] W. W. True and K. W. Ford, Phys. Rev. **109**, 1675 (1958).

language of the shell model. Since, in nuclear spectroscopy, one would study particles scattered from a particular excited state of the nucleus, the target nucleus is described by a closed-shell core plus those extra-core nucleons which characterize the ground and excited states of interest. Such extra-core nucleons are represented by harmonic oscillator radial functions with angular momentum and spin coupled to give a proper shell-model description in terms of the quantum numbers n, l, j, m, where n is the principal quantum number, l is the orbital angular momentum, j the total angular momentum, and m its z component. When more than one nucleon lies beyond the core, they are represented by a properly antisymmetric wave function with total angular momentum equal to that of the nucleus.

The free nucleon, both before and after the direct interaction takes place, is subject to elastic scattering and partial absorption by the entire nucleus. Because of the success of the optical model in describing the elastic scattering of nucleons by complex nuclei,[12–14,21,22] the free particle is represented by the wave function of a particle moving in the presence of a complex potential well. For simplicity a square well is used rather than a rounded well. A few calculations with rounded wells have been made, and are discussed in Sec. V.

The direct interaction between free and bound nucleons is chosen to have a Gaussian form, and is spin-independent. In accordance with the assumption of a surface interaction, the direct two-body interaction has the form

$$V_d(|\mathbf{r}_1-\mathbf{r}_2|)=\gamma\delta(r_1-r_0)U_d(|\mathbf{r}_1-\mathbf{r}_2|), \qquad (2)$$

where γ has the dimension of length and is introduced so that U_d has the dimension of energy. The coordinate $\mathbf{r}_1$ refers to the free nucleon and $\mathbf{r}_2$ to the bound nucleon, and r_0 is the interaction radius.

Our choice of shell-model wave functions and two-body interaction is the one usually adopted in shell-model calculation.[20,23]

The above description of the direct interaction process is illustrated schematically in Fig. 1.

The cross section is calculated in first-order perturbation theory.[24] That is

$$\sigma(\theta)=\frac{k'}{k}\left(\frac{m}{2\pi\hbar^2}\right)^2|\mathfrak{M}|^2, \qquad (3)$$

where k and k' are, respectively, the incident and outgoing propagation numbers, m is the reduced mass of the projectile, and $\mathfrak{M}$ is the matrix element of the direct interaction taken between the initial and final states of the system.

[21] R. D. Woods and D. S. Saxon, Phys. Rev. **95**, 577 (1954).
[22] Beyster, Walt, and Salmi, Phys. Rev. **104**, 1319 (1956).
[23] I. Talmi, Helv. Phys. Acta **25**, 185 (1952).
[24] N. F. Mott and H. S. W. Massey, *The Theory of Atomic Collisions* (Oxford University Press, London, 1949), second edition.

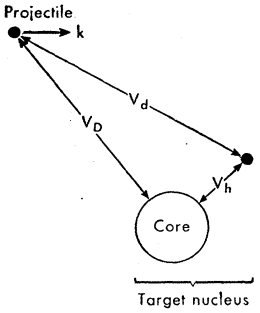

FIG. 1. Schematic representation of the direct-interaction scattering. V_h is the harmonic oscillator potential in which the extra-core nucleon moves. V_D is the distorting potential representing the interaction of the projectile with the whole nucleus, and V_d is the direct potential acting between extra-core nucleon and projectile which gives rise to the inelastic scattering.

2. Scattering from Nuclei with One Extra-Core Nucleon

For illustrative purposes we suppose that the ground state and excited state of a certain nucleus can be described as a zero-spin core plus one nucleon. (Other cases are mentioned briefly in the Appendix.) Hence the direct interaction will be diagonal with respect to the wave function of the core particles, so that the nuclear wave function need contain a description of only the extra-core particle. As a result of the direct interaction the extra-core nucleon becomes excited so that its quantum numbers change,

$$nljm \rightarrow n'l'j'm'.$$

For the wave function of the extra-core particle we write

$$|nljm\rangle=R_{nl}(r)|ljm\rangle, \qquad (4)$$

where R_{nl} is the radial function and $|ljm\rangle$ is the spin-angle function:

$$|ljm\rangle=\sum_{m_l m_s} C(lsj;m_l m_s m)|lm_l\rangle|sm_s\rangle. \qquad (5)$$

Here $C(j_1 j_2 j;m_1 m_2 m)$ is a Clebsch-Gordan coefficient, $|sm_s\rangle$ is a spin function, and

$$|lm_l\rangle=Y_l^{m_l}(\theta,\phi)$$

is a spherical harmonic. The free particle can be regarded as spinless, since we use a spin-independent interaction. Since the free particle is regarded as moving in the field of a complex distorting potential, its expansion in partial waves is written

$$|\mathbf{k}\rangle=\sum_p\{4\pi(2p+1)\}^{\frac{1}{2}}i^p f_p(kr)|p0\rangle, \qquad (6)$$

where $\mathbf{k}$ has been chosen to define the direction of the polar axis, $|p0\rangle$ is a spherical harmonic, and the radial functions $f_p(kr)$ are solutions of the equation

$$\left(\frac{1}{r}\frac{d^2}{dr^2}r-\frac{l(l+1)}{r^2}-\frac{2m}{\hbar^2}V_D(r)+k^2\right)f_l=0, \qquad (7)$$

V_D is the distorting potential and

$$k^2=(2m/\hbar^2)E, \tag{8}$$

where E is the relative energy of the incident particle. If $V_D\equiv 0$ then $f_l(kr)=j_l(kr)$, where j_l is a spherical Bessel function. In general the emitted particle emerges in a direction different from $\mathbf{k}$. Therefore we write

$$\langle \mathbf{k}'| = 4\pi \sum_{p'\mu} (-i)^{p'} f_{p'}(k'r)\langle p'\mu| Y_{p'}{}^{\mu}(\hat{k}'). \tag{9}$$

Notice that although f_l is a complex valued function, its complex conjugate does not appear in the expression for $\langle \mathbf{k}|$ (see reference 24, p. 144). Indeed $\langle \mathbf{k}|$ is not, strictly speaking, the adjoint of $|\mathbf{k}\rangle$.

The initial and final state of the system can now be written down,

$$|i\rangle = (4\pi)^{\frac{1}{2}} \sum_p i^p (2p+1)^{\frac{1}{2}} f_p(kr_1) R_{nl}(r_2) |p0\rangle_1 |ljm\rangle_2,$$

$$\langle f| = 4\pi \sum_{p'\mu} (-i)^{p'} f_{p'}(k'r_1) R_{n'l'}(r_2) Y_{p'}{}^{\mu}(\hat{k}') \langle p'\mu|_1 \times \langle l'j'm'|_2. \tag{10}$$

The direct interaction is developed in its angular momentum transfer operators $v_L(r_1,r_2)$;

$$V_d(|\mathbf{r}_1-\mathbf{r}_2|) = \sum_L v_L(r_1,r_2) P_L(\cos\theta_{12}) = \sum_L \frac{4\pi}{2L+1} v_L(r_1,r_2) \sum_M (-)^M Y_L{}^M(1) Y_L{}^{-M}(2). \tag{11}$$

The matrix element of this interaction is

$$\mathfrak{M} = \langle f|v|i\rangle = (4\pi)^{\frac{1}{2}} \sum_{pp'L} \sum_{M\mu} (-)^M i^{p-p'} (2p+1)^{\frac{1}{2}} Y_{p'}{}^{\mu}(\hat{k}') \times R_{p'Lp} \langle p'\mu| Y_L{}^{-M}|p0\rangle \langle l'j'm'| Y_L{}^M |ljm\rangle, \tag{12}$$

where

$$R_{p'Lp} = \frac{1}{2L+1} \int\int dr_1 dr_2 r_1^2 r_2^2 f_{p'}(k'r_1) R_{n'l'}{}^*(r_2) \times v_L(r_1,r_2) f_p(kr_1) R_{nl}(r_2). \tag{13}$$

We shall show later how this radial integral can be explicitly evaluated for the particular choice of functions that we have made.

The Wigner-Eckart theorem[25] gives us

$$\langle l'j'm'| Y_L{}^M |ljm\rangle = C(jLj';mMm') \langle l'j'\| Y_L \| lj\rangle. \tag{14}$$

Using methods developed by Racah[26] we find

$$\langle l'j'\| Y_L \| lj\rangle = (-)^{\frac{1}{2}+L-l-j'} \{(2l'+1)(2j+1)\}^{\frac{1}{2}} \times W(ljl'j';\tfrac{1}{2}L) (l'\| Y_L \| l), \tag{15}$$

also

$$\langle p'\mu| Y_L{}^{-M}|p0\rangle = C(pLp;0-M\mu)(p'\| Y_L \| p), \tag{16}$$

where

$$(l'\| Y_L \| l) = \left[\frac{(2l+1)(2L+1)}{4\pi(2l'+1)}\right]^{\frac{1}{2}} C(lLl';000). \tag{17}$$

Rose's definition of reduced matrix elements is used here.[25] The connection with Racah's is

$$\langle j\| T_L \| j'\rangle_{\text{Racah}} = (2j+1)^{\frac{1}{2}} \langle j\| T_L \| j'\rangle_{\text{Rose}}. \tag{18}$$

Ford[17] has pointed out that the reduced matrix element $\langle l'j'\| Y_L \| lj\rangle$ can be written in a particularly simple form,

$$\langle l'j'\| Y_L \| lj\rangle = \left[\frac{(2L+1)(2j+1)}{4\pi(2j'+1)}\right]^{\frac{1}{2}} C(jLj';-\tfrac{1}{2}0-\tfrac{1}{2}), \quad \text{for} \quad l+l'+L\equiv\text{even}$$
$$= 0, \quad \text{for} \quad l+l'+L\equiv\text{odd}. \tag{19}$$

Using the results given above, one obtains

$$\mathfrak{M} = (4\pi)^{\frac{3}{2}} (-)^{\frac{1}{2}+L-l-j'} \{(2l+1)(2j+1)\}^{\frac{1}{2}} \sum_{pp'L} i^{p-p'} \frac{2p+1}{(2p'+1)^{\frac{1}{2}}} (2L+1) R_{p'Lp} C(lLl';000) C(pLp';000) W(ljl'j';\tfrac{1}{2}L) \sum_M C(pLp';0MM) C(jLj';m-Mm') Y_{p'}{}^{M*}(\hat{k}'). \tag{20}$$

The cross section is given in terms of $\mathfrak{M}$ by

$$\sigma(\theta) = \frac{k'}{k} \left(\frac{m}{2\pi\hbar^2}\right)^2 \sum_{\text{Av}} |\mathfrak{M}|^2, \tag{21}$$

where

$$\sum_{\text{Av}} \rightarrow \frac{1}{2j+1} \sum_{m,m'}$$

[25] M. E. Rose, *Elementary Theory of Angular Momentum* (Jonh Wiley and Sons, Inc., New York, 1957).
[26] G. Racah, Phys. Rev. **62**, 438 (1942); **63**, 367 (1943).

is a sum over final spin directions m' and an average over the initial directions m. Notice that $\sum_{\text{Av}}|\mathfrak{M}|^2$ contains the sum

$$\sum_{m,m'} C(jLj';\, m-Mm')C(jL'j';\, m-M'm')=\frac{2j'+1}{2L+1}\delta_{LL'}\delta_{MM'}, \tag{22}$$

where L' and M' enter through squaring the sum (20). Thus one can write

$$\sum_{\text{Av}}|\mathfrak{M}|^2=(4\pi)^{\frac{3}{2}}(2l+1)(2j'+1)\sum_{pp'qq'L} i^{p-p'-q+q'}\frac{(2p+1)(2q+1)}{\{(2p'+1)(2q'+1)\}^{\frac{1}{2}}}$$
$$\times C^2(lL l';\,000)(2L+1)R_{p'Lp}R^*_{q'Lq}C(pLp';\,000)C(qLq';\,000)$$
$$\times W^2(ljl'j';\,\tfrac{1}{2}L)\sum_M (-)^M C(pLp';\,0MM)C(qLq';\,0MM)Y_{p'}{}^M(\hat{k}')Y_{q'}{}^{-M}(\hat{k}'). \tag{23}$$

where q and q' are the annalogs of p and p' that enter when the square of the sum (20) is formed. The sum over M can be performed first by writing the product $Y_{p'}{}^M Y_{q'}{}^{-M}$ as a series of spherical harmonics (see, for example, Blatt and Weisskopf[27].) The sum over M now involves the product of three Clebsch-Gordan coefficients. This can be summed by standard methods.[25] One obtains

$$\sum_M (-)^M C(pLp';\,0MM)C(qLq';\,0MM)Y_{p'}{}^M(\hat{k}')Y_{q'}{}^{-M}(\hat{k}')$$
$$=\frac{(2p'+1)(2q'+1)}{4\pi}(-)^L\sum_n C(pqn;\,000)C(p'q'n;\,000)W(pp'qq';\,Ln)P_n(\cos\theta), \tag{24}$$

where θ is the polar angle of $\mathbf{k}'$. This result is of course independent of ϕ.

Introduce the Z coefficient defined by

$$Z(abcd;\,ef)=\{(2a+1)(2b+1)(2c+1)(2d+1)\}^{\frac{1}{2}}C(acf;\,000)W(abcd;\,ef), \tag{25}$$

and observe that we can replace $(-)^L$ by $(-)^{q+q'}$ by virtue of $C(qLq';\,000)$. Then the differential cross section can be written

$$\sigma(\theta)=\frac{k'}{k}\left(\frac{2m}{\hbar^2}\right)^2\frac{1}{2j+1}\sum_{pp'qq'}\sum_{Ln} i^{p-p'+q-q'}\{(2p'+1)(2q'+1)\}^{\frac{1}{2}}$$
$$\times(2p+1)(2q+1)R_{p'Lp}R^*_{q'Lq}C(pLp';\,000)C(qLq';\,000)$$
$$\times C(pqn;\,000)C(p'q'n;\,000)Z^2(ljl'j';\,\tfrac{1}{2}L)W(pp'qq';\,Ln)P_n(\cos\theta) \tag{26}$$

For calculation purposes it is useful to note

$$Z(ljl'j';\,\tfrac{1}{2}L)=0, \quad \text{for} \quad l+l'+L\equiv\text{odd}, \quad \text{otherwise}$$
$$=(-)^{j-\frac{1}{2}}\{(2L+1)(2j+1)\}^{\frac{1}{2}}C(jLj';\,\tfrac{1}{2}0\tfrac{1}{2}). \tag{27}$$

The integrated cross section is

$$\sigma=4\pi\frac{k'}{k}\left(\frac{2m}{\hbar^2}\right)^2\frac{1}{2j+1}\sum_{pp'L}(2p+1)C^2(pLp';\,000)Z^2(ljl'j';\,\tfrac{1}{2}L)\,|R_{p'Lp}|^2 \tag{28}$$

The factor $Z(ljl'j';\,\frac{1}{2}L)$ carries the selection rules on L which is the index on the angular momentum transfer operator, Eq. (11),

$$l+l'+L\equiv\text{even},$$
$$\mathbf{l}+\mathbf{l}'+\mathbf{L}=0, \tag{29}$$
$$\mathbf{j}+\mathbf{j}'+\mathbf{L}=0.$$

If the target nucleus has zero spin then there is the additional selection rule

$$L=J, \tag{30}$$

where J is the spin of the final nucleus.

[27] J. M. Blatt and V. F. Weisskopf, *Theoretical Nuclear Physics* (John Wiley and Sons, Inc., 1952), p. 793.

Notice that the first of the selection rules above states that the parity change of the nucleus is $(-)^L$, so that for even-even nuclei, only states of even spin, even parity, or odd spin, odd parity can be excited in our theory by direct-interaction scattering. Excitation of the other states requires a spin flip between incident and emitted particle.

3. Integration of the Radial Coordinates

We now show how the integration of the variable r_2 can be performed in $R_{p'Lp}$ [Eq. (13)] for the particular choice of functions made here. The interaction potential is assumed to be Gaussian, so that we have

$$\begin{aligned} V_d &= -V_0 \exp(-\beta|\mathbf{r}_1-\mathbf{r}_2|^2) \\ &= -V_0 \exp[-\beta(r_1^2+r_2^2)] \textstyle\sum_L (2L+1) i^L j_L(-2i\beta r_1 r_2) P_L(\mu), \end{aligned} \tag{31}$$

where $\mu=\cos\theta_{12}$. Hence

$$v_L(r_1,r_2) = -(2L+1) i^L V_0 j_L(-2i\beta r_1 r_2) \exp[-\beta(r_1^2+r_2^2)] \tag{32}$$

leading to

$$R_{p'Lp} = -i^L V_0 \int_0^\infty dr_1\, r_1^2 f_p(kr_1) f_{p'}(k'r_1) \exp(-\beta r_1^2) \int_0^\infty dr_2\, r_2^2 R^*_{n'l'}(r_2) \exp(-\beta r_2^2) j_L(-2i\beta r_1 r_2) R_{nl}(r_2). \tag{33}$$

For the bound-state radial functions R_{nl}, the oscillator functions are used,

$$\begin{aligned} R_{nl}(r) &= N_{nl} \nu^{\frac{3}{4}} (\nu^{\frac{1}{2}} r)^l \exp(-\tfrac{1}{2}\nu r^2) \sum_{k=0}^{n-1} \binom{n-1}{k} \frac{(2l+1)!!}{(2l+2k+1)!!} (-2\nu r^2)^k, \\ N_{nl}^2 &= 2^{2(l-n+2)} \pi^{-\frac{1}{2}} \frac{(2l+2n-1)!}{(n-1)!(l+n-1)!} \left[\frac{l!}{(2l+1)!}\right]^2. \end{aligned} \tag{34}$$

(The lowest oscillator state is given by $n=1$ in this notation.) Therefore we write

$$R_{nl} R_{n'l'} = N_{nl} N_{n'l'} \nu^{\frac{3}{2}} (\nu^{\frac{1}{2}} r)^{l+l'} \exp(-\nu r^2) \sum_{k=1}^{n+n'-1} \alpha_k (\nu r^2)^{k-1}, \tag{35}$$

where α_k depends on $nln'l'$ except $\alpha_1 \equiv 1$, and is defined by referring to the explicit form of R_{nl}. Introduce the dimensionless quantities

$$y = \nu^{\frac{1}{2}} r_2, \quad b = -2i\beta\nu^{-\frac{1}{2}} r_1. \tag{36}$$

Then

$$\begin{aligned} R_{p'Lp} = -i^L V_0 N_{nl} N_{n'l'} &\int_0^\infty dr_1\, r_1^2 f_{p'}(k'r_1) \exp(-\beta r_1^2) f_p(kr_1) \\ &\times \int_0^\infty dy\, y^{l+l'+2} j_L(by) \exp\left[-\frac{\beta+\nu}{\nu} y^2\right] \sum_{k=1}^{n+n'-1} \alpha_k y^{2(k-1)}. \end{aligned} \tag{37}$$

Call

$$s = l+l'+2(k-1), \quad \rho = \nu/(\beta+\nu). \tag{38}$$

Then the integral over y is

$$G_L(s) = \int_0^\infty dy\, y^{s+2} j_L(by) \exp(-y^2/\rho). \tag{39}$$

Konopinski[28] has illustrated the use of the following result in evaluating Slater integrals:

$$\int_0^\infty J_\nu(ar) \exp(-p^2 r^2) r^2 dr = \frac{a^\nu}{(2p^2)^{\nu+1}} \exp\{-(a/2p)^2\}, \tag{40}$$

which of course can be rewritten in terms of j_L. To arrange for the appropriate power of y to appear in $G_L(s)$ so that Eq. (40) can be applied, use the fact that differentiation by $(\rho^2\partial/\partial\rho)^n$ introduces the factor y^{2n} into the integrand. Then

$$G_L(s) = \frac{\pi b^L}{2^{L+2}} \left(\rho^2 \frac{\partial}{\partial\rho}\right)^{\frac{1}{2}(s-L)} \rho^{L+\frac{3}{2}} \exp\{-b^2\rho/4\}. \tag{41}$$

[28] E. J. Konopinski, Indiana University (private communication).

Note that s-L is always an even integer because

$$2g=l+l'+L=\text{even},$$

as required by the factor $C(lLl';000)$ appearing in the cross section.

This completes the integration of the variable r_2. The integration over r_1 can be done explicitly if we make the assumption that the direct interaction takes place when the incident nucleon lies on some interaction surface of radius r_0. For this purpose we insert the factor $\gamma\delta(r_1-r_0)$ into the r_1 integration (γ has the dimension of length). The result is

$$R_{p'Lp}=-\frac{\pi^{\frac{1}{2}}}{4}(V_0\gamma r_0^2)N_{nl}N_{n'l'}f_{p'}(k'r_0)f_p(kr_0)\left(\frac{\beta r_0}{\nu^{\frac{1}{2}}}\right)^L\sum_{k=1}^{n+n'-1}\alpha_k g_k(ll';L), \tag{42}$$

where

$$g_k(ll';L)=\left(\rho^2\frac{\partial}{\partial\rho}\right)^{g-L+k-1}\rho^{L+\frac{3}{2}}\exp\{-(1-\rho\beta/\nu)\beta r_0^2\}. \tag{43}$$

4. Properties of the Surface-Reaction Model of Direct-Interaction Scattering

It is shown here that if the direct interaction is a surface phenomenon then the shapes of the angular distribution and excitation function of the inelastically scattered particles are rather insensitive to the force range of the direct interaction, to the radial parameter ν of the bound radial function, and to the single-particle quantum numbers nlj of the bound nucleon, except as they determine the allowed angular-momentum transfer numbers L.

For a surface interaction as defined by Eq. (2) the radial factor $R_{p'Lp}$, which appears in the expression for the cross section, can be written

$$R_{p'Lp}=\gamma r_0^2 f_p(kr_0)f_{p'}(k'r_0)\frac{1}{2L+1}\times\int_0^\infty dr\, r^2R_{n'l'}{}^*(r)v_L(r_0,r)R_{nl}(r), \tag{44}$$

where the notation of Sec. IV-2 has been used. Thus the surface interaction causes a factorization of $R_{p'Lp}$ in its dependence on its indices. Referring to expression (26) for the angular distribution, one sees that as a consequence the cross section has the form

$$\sigma(\theta)=\sum_L a_L(\beta,\nu)\sum_m b_{Lm}(k,k')P_m(\cos\theta), \tag{45}$$

where

$$a_L=a_L(nlj;n'l'j'|\beta\nu)$$

is a function of those quantities to which the cross section is stated to be insensitive, and

$$b_{Lm}=b_{Lm}(V,W,R|kk')$$

is a function of the optical-model distorting potential whose parameters are denoted by V, W, and R, the real and imaginary well depths and radius, respectively.

One expects that when more than one L is allowed by the selection rules, the smallest one, say λ, gives the largest contribution to the sum. Therefore we can write approximately

$$\sigma(\theta)\simeq a_\lambda(\beta,\nu)\sum_m b_{\lambda m}(k,k')P_m(\cos\theta). \tag{46}$$

For an even-even nucleus, only one L is allowed, namely $L=J$. Only one term appears in the sum, and no approximation is implied in writing Eq. (46) in this case. Thus we see that the function a_L becomes merely a multiplicative factor, and the assertion made above is true.

The foregoing discussion is valid in the limit of a surface interaction. Such an interaction is of course an idealization. Physically one would expect the interaction to occur throughout some region of finite extension near the nuclear surface under those circumstances where a surface interaction is expected. Even so the thickness of this region may be too small to allow the incident nucleon to react sensitively to the radial state of the bound nucleon. Moreover, if the interaction region lies in the region in which the bound particles are represented by exponential tails, it is clear that the shapes (but not the absolute magnitudes) of the cross sections are insensitive to the single-particle transition in the nucleus.

V. STUDY OF THE APPROXIMATIONS

Several approximations have been made in calculating the cross section for direct-interaction inelastic scattering of nucleons by complex nuclei. We here attempt to establish the significance of these approximations.

1. Square-Well Distorting Potential

It is well known that a significant improvement in the fit to elastic nucleon-scattering data was obtained when the edge of the square-well optical potential was rounded.[21] Nevertheless, because of the increased calculating time that use of a rounded optical potential would require, a complex square well was used as the distorting potential in the calculations for this paper. However, several sample calculations were performed with a rounded well, to ascertain the effect of the rounded edge.

It should be noted that a potential with a rounded edge tends to cause less reflection of the incident waves at the edge of the potential than a square well. Accordingly, a square well that gives reflection at the edge

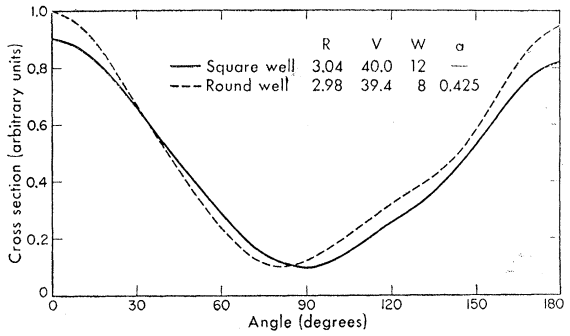

FIG. 2. Comparison of calculated direct surface-interaction angular distributions. of 15.2-Mev (lab) neutrons scattered from the 4.43-Mev level in carbon using a Saxon well and a square-well complex distorting potential. The cross sections are normalized at their minima. Lengths are quoted in units of 10^{-13} cm and energies in Mev.

comparable to a Saxon-type optical potential requires a deeper imaginary well depth than the Saxon potential.

In Fig. 2 a comparison is made between the angular distribution calculated from the surface-interaction model, using a square and a rounded-edge complex distorting potential, for inelastic scattering of 15.2-Mev (lab) neutrons from the 4.43-Mev level in C^{12}.

This particular calculation agrees only qualitatively with the experimental data, and is presented to indicate to what degree the parameters defining a square well can be chosen to yield a cross section similar to that calculated with a particular set of Saxon-well parameters. The shapes of the angular distributions agree quite well, although the total cross section for the rounded-well calculation is about 5.5 times that for the square well.

It appears therefore that, by a suitable increase of the imaginary part of the potential, the square distorting potential can be made to yield the same shape of inelastic angular distribution as the rounded well, but with a change in the magnitude of the predicted cross section by as much as a factor of 6. Therefore, the use of the square well, with results suitably renormalized, has the advantage of saving a substantial amount of calculating time without sacrificing the ability to fit experimental cross sections. On the other hand, it has the disadvantage that it does not accurately predict elastic angular distributions, so that elastic and inelastic scattering are not fitted into a single consistent model.

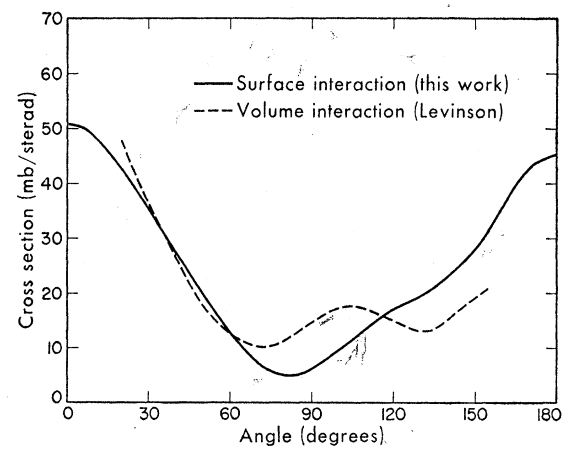

FIG. 3. Angular distribution of 14-Mev nucleons inelastically scattered from the 4.43-Mev level in C^{12}. Curves compare the Levinson-Banerjee calculation with the surface-interaction model of this work, in which the same Saxon well potential was used for the distorting potential. An interaction radius of 3.3×10^{-13} cm was used in the surface-interaction model. The Saxon well parameters are listed in Fig. 2.

2. Surface Interaction

Reasons have been given in Sec. III for expecting that a surface interaction for direct reactions may be a good approximation for a suitable range of incident energies. Levinson and Banerjee[5] calculated the inelastic cross section for 14-Mev protons on the 4.43-Mev level of C^{12}, using a rounded-edge distorting potential, and a volume interaction. This is compared in Fig. 3 with a calculation for a surface interaction based on the same distorting potential, except that the Coulomb repulsion is not included. For the latter calculation an interaction radius was used that is larger by about 10% than the radius of the Saxon potential. Considering how sensitive the cross sections are to the optical-model parameters (Sec. VI), the agreement is quite satisfactory. It indicates that the main contribution of the volume interaction used by Levinson and Banerjee comes from the surface region, and corroborates our use of a surface interaction. Moreover, the agreement implies, as earlier discussed, that the shape of the cross sections is determined principally by the optical-model parameters and by the allowed angular-momentum transfer numbers L; not by the particle quantum numbers.

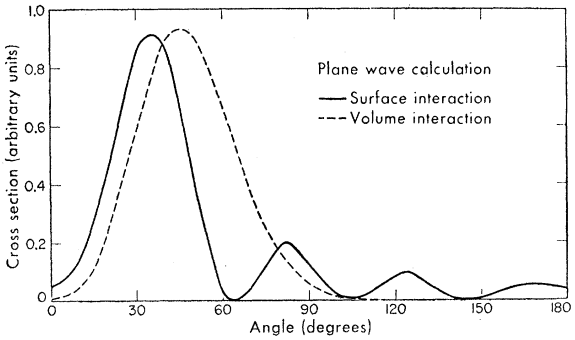

FIG. 4. Angular distribution of 31.5-Mev alpha particles scattered from the 4.43-Mev level in C^{12}. The curves compare a surface and volume direct-interaction model in the plane-wave Born approximation. The curves are arbitrarily normalized. For the surface interaction, the interaction radius is 5.9×10^{-13} cm.

A comparison is made in Fig. 4 between plane-wave calculations for 31.5-Mev alpha-particle inelastic scattering from the 4.43-Mev level in carbon.[29] Here of

[29] H. J. Watters, Phys. Rev. **103**, 1763 (1956).

course the free-nucleon wave function is not damped inside the nucleus, as it is for a function distorted by a complex potential. As one might expect, the volume interaction shows little trace of the diffraction minima present in the surface-interaction angular distribution. The volume interaction also reduces markedly the scattering at larger angles, compared with the first peak at small angle.

3. Exchange Forces

Throughout this work, a nonexchange force has been used for the direct interaction. In addition, the wave function describing the system of incident nucleon plus bound nucleons has not been antisymmetrized with respect to interchange of the free nucleon with one of the bound nucleons, as required when all are identical nucleons. Both the exchange force and antisymmetrization of the wave function have similar consequences, so that we make no distinction between them in the discussion of their omission.

Antisymmetrization gives rise to exchange integrals. Therefore it is appropriate to examine the relative magnitudes of the direct and exchange terms, which have the form

$$D=(f_{p'}(r_1)R_{l'}(r_2),\ V_{12}f_p(r_1)R_l(r_2)),$$
$$E=(f_{p'}(r_2)R_{l'}(r_1),\ V_{12}f_p(r_1)R_l(r_2)).$$

These integrals are quite sensitive to the degree of overlap of the radial functions. The exchange integral generally contains poorer overlap because a bound radial function is associated with a free-particle radial function, and the latter decays with an exponential amplitude inside the nucleus. Indeed, the calculation by Levinson and Banerjee[5] for C^{12} indicates that the exchange contribution is very small.

For a zero-range interaction, the exchange contribution is precisely zero. For, in this case, the two nucleons can interact only in the symmetric space state because the direct and exchange integrals are equal. The matrix element of the interaction accordingly is proportional to $2D$. The statistical weight of the space-symmetric state is, however, $\frac{1}{4}$. Hence the cross section is proportional to $|D|^2$. This result is equivalent to that which would be obtained if nonsymmetrized functions were used from the beginning.

In the limit that the direct interaction becomes strictly a surface interaction as defined in Sec. IV, the shapes of the cross sections, both total and differential, become insensitive to the range of the direct interaction. In particular, for a zero-range force the cross section is independent of the symmetrization. Therefore, in the limit of a surface interaction, the shape of the cross section is approximately independent of the exchange character of the interaction and of the possibility of exchange collisions between identical nucleons.

TABLE I. Percentage admixtures of the dominant configurations in several states of Pb^{206}.[a]

Energy of level (Mev)	Spin	Percentage admixture $(p_{1/2})^{-2}$	$(p_{1/2}f_{5/2})^{-1}$	$(p_{1/2}p_{3/2})^{-1}$
0	0+	73	0	0
0.803	2+	0	56	30
1.45	2+	0	37	60

[a] See reference 20.

4. Pure Shell-Model States

Throughout the calculations in this work, pure shell-model wave functions have been used to describe the bound nucleons. If one were to admit configuration mixing, interference terms would appear in the cross section, and these cannot be evaluated as concisely as has been done for the pure states. The justification for use of pure states is that certain of the states of the residual nucleus are excited with far greater probability than others. Such states are those whose overlap with the initial stage is large.

Consider, as an example, excitation of the 2+ states at 0.803 and 1.45 Mev in Pb^{206}. The dominant configuration admixtures for the states involved found by True and Ford[20] are listed in Table I. The excited states are seen to contain large impurities. However, the calculated cross sections for direct-interaction inelastic scattering, which cause the single-particle transitions

$$3p_{\frac{3}{2}} \rightarrow 3p_{\frac{1}{2}},$$
$$2f_{\frac{5}{2}} \rightarrow 3p_{\frac{1}{2}},$$

differ by a factor of 100 in favor of the first. The relative cross sections which lead to the final configurations shown are listed in Table II. It is evident that the excitation of both 2+ levels is due to the same configuration component, and this component is excited with a cross section large enough that the other components and interference terms contribute negligibly.

In summary, it appears that none of the approximations introduced in our calculations introduces serious errors, except for the error in magnitude, which can be corrected by a renormalizing factor. It should be possible with the model considered here to calculate angular distributions for inelastic scattering nearly as accurately as in a refined model which includes a rounded complex well, a volume interaction, exchange forces, and mixed configurations—refinements, however, which would greatly lengthen the calculating time.

TABLE II. Calculated relative cross sections for excitation of the dominant configurations in the two low-lying 2+ states of Pb^{206}.

Energy of level (Mev)	Relative cross section $(p_{1/2}f_{5/2})^{-1}$	$(p_{1/2}p_{3/2})^{-1}$
0.803	1×10^{-2}	1
1.45	4×10^{-3}	4×10^{-1}

VI. GENERAL STUDY

We wish here to report a few calculations for inelastic scattering of 15-Mev neutrons from a hypothetical nucleus ($A\sim30$) to illustrate the sensitivity of the cross sections to assumptions about the target. For this purpose, we adopt as standard parameters the following:

Energy of excited state,	$E_L=2$ Mev,
Real depth of square well,	$V=-40$ Mev,
Imaginary depth of square well,	$W=-12$ Mev,
Radius of square well,	$R=4\times10^{-13}$ cm,
Interaction radius,	$R_I=R$.

In Fig. 5 we compare cross sections for various assumptions about the levels. Two curves correspond to an even-even nucleus with two nucleons beyond doubly closed shells. (Except for a multiplicative factor this is the same as for closed shells.) The curves corresponding to a 2+ and a 4+ excited state show a marked difference in character. This suggests that the analysis of inelastic scattering may be a useful tool in determining the spin and parities of nuclear states, provided that in the same nucleus one or more known levels may be successfully analyzed to provide the parameters of the distorting potential. Contrast these curves calculated in the distorted-wave approximation with the plane-wave result, which for the 2+ state is just $j_2^2(QR)$. The latter predicts negligible scattering in the forward direction, and is smoother than the cross sections calculated in the distorted-wave approximation. This comparison illustrates the dominant role played by the distortion of the incident and emitted waves by the nucleus. The remaining curve on this figure is calculated for an odd-even nucleus having a single nucleon beyond a zero-spin core. The single-particle transition is $d_{\frac{5}{2}}\rightarrow g_{\frac{7}{2}}$, which allows angular-momentum transfers $L=2$, 4, and 6. This cross section is very similar to the $0+\rightarrow 2+$ transition in even-even nuclei because the $L=2$ component is larger than the $L=4$ or 6 components.

In Fig. 6 two cross sections are calculated under the same circumstances except that the excited state is at 2 Mev for the one calculation, and 4 Mev for the other. The curves are very similar, and probably this is generally true as long as the energy of the excited state is small compared with the incident energy. The magnitude of the cross section is somewhat reduced for the higher excited state, as expected from overlap consideration.

In Fig. 7 we compare the angular distributions of neutrons inelastically scattered from even-even nuclei having several different radii. Curves with constant VR^2 and WR^2 are similar, so that similar results would be obtained by changing the depth of the distorting potentials. These curves exhibit marked differences, illustrating once again the dominant role played by the distorting potential in determining the inelastic scattering.

Figure 8 shows cross sections resulting from excitation of odd-parity states in even-even nuclei. These cross sections are small at forward angles, in contrast to the forward peaking found in most calculations with no parity change (Fig. 5 and 7). This qualitative difference suggests that the parity change may be determined experimentally by a very cursory examination of the angular distribution. It is intended that a closer study of this matter will be made at a later date.

We compare, in Fig. 9, calculations made by using several values of the interaction radius R_I and imaginary part W of the distorting potential. Increasing either R_I or W tends to reduce the back-angle scattering relative to scattering in the forward hemisphere. If W is varied over a reasonable range of values, the direct-interaction inelastic cross section decreases as W increases, while the cross section for compound-nucleus formation increases, or—more precisely—the cross section for all other inelastic processes increases.

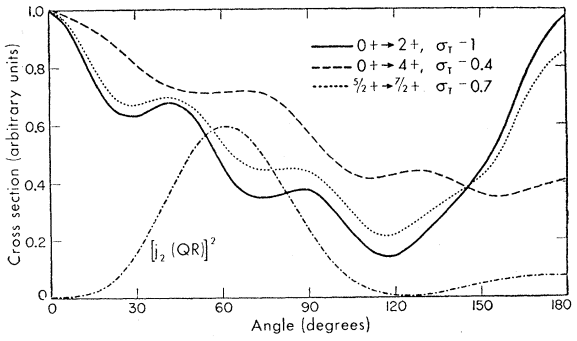

FIG. 5. Angular distribution of 15-Mev neutrons inelastically scattered from a nucleus ($A\sim30$). The 0→2 and 0→4 curves are for an even-even nucleus with ground- and excited-state spins and parities as indicated. The $\frac{5}{2}\rightarrow\frac{7}{2}$ curve is for an odd-even nucleus which allows angular momentum transfers 2, 4, and 6. The σ_T indicates relative total cross sections when there are two nucleons beyond closed shells in the even-even nuclei.

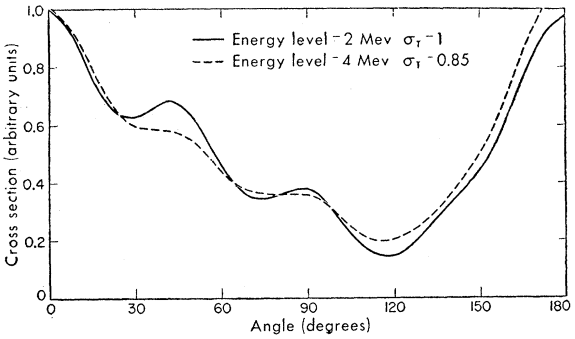

FIG. 6. Angular distribution of 15-Mev neutrons inelastically scattered from an even-even nucleus ($A\sim30$). The curves correspond to states at 2 and 4 Mev, respectively. The single-particle transition is the same in both cases and the spin change is $0+\rightarrow 2+$.

VII. COMPARISON OF THEORY WITH EXPERIMENT

I. Introduction

In the preceding sections a model for the description of nucleon inelastic scattering by direct interaction with a bound nucleon has been presented. The calculations reported below apply to uncharged particles, because Coulomb distortion of the incident waves has not been included. However, Levinson and Banerjee found for proton scattering on C^{12} that the Coulomb distortion played a very minor role in determining the angular distributions for incident energies greater than about 16 Mev. Because of this finding, and the fact that there is a dearth of experimental measurements of neutron angular distributions from resolved final states, we include a comparison of the present theory with charged-particle inelastic scattering.

2. Choice of Nuclear Parameters

It was pointed out earlier that, in the model of inelastic scattering presented here, the shapes of the cross sections are almost independent of the parameters β, ν, and V_0, the depth of the direct interaction. The choice of values for these parameters is therefore not critical.

The direct interaction parameters V_0 and β are chosen to be those which yield the correct n-n low-energy scattering in singlet even states.

$$V_0=-32.5 \text{ Mev},$$
$$\beta=0.2922\times(10^{-13} \text{ cm})^{-2}.$$

The parameter ν which appears in the oscillator radial function $[\psi\sim\exp(-\frac{1}{2}\nu r^2)]$ is determined by requiring the classical turning point in the oscillator potential to lie at some reasonable radius R_0. In particular we shall often choose R_0 to be the radius of the Saxon well at which a nucleon in the S state would be bound with energy of $B=10$ Mev. Let N_0 be the oscillator quantum number $[N_0=2(n-1)+l]$, which determines, the energy of the oscillator state, $E=(N_0+3/2)\hbar\omega$. At the classical turning point we have

$$(N_0+3/2)\hbar\omega=V(R_0)=(1/2)M\omega^2R_0^2.$$

Since $\nu=M\omega/\hbar$, then

$$\nu=(2N_0+3)/R_0^2.$$

Since, however, only one value of ν can be used conveniently in the theory, we choose ν to be the same for both initial and final single-particle states, and equal to

$$\nu=(N_0+N_0'+3)/R_0^2.$$

In seeking to fit the theory to experimental angular distributions, the usual procedure adopted was to choose the radius R of the square-well distorting potential to be approximately equal to that given by elastic scattering data, and then to adjust V and W for a best fit, where

$$V_{\text{distorting}}=V+iW, \quad \text{for} \quad r<R$$
$$=0, \quad \text{for} \quad r>R.$$

The analysis of neutron elastic scattering by Beyster

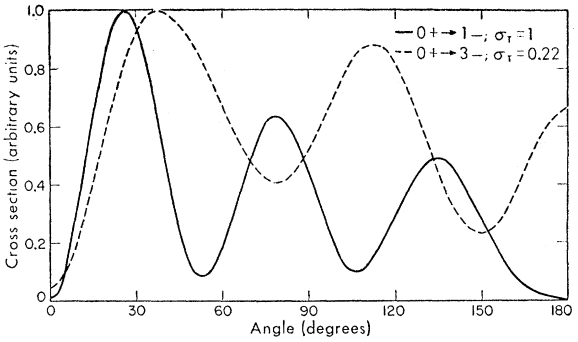

FIG. 8. Angular distribution of 15-Mev neutrons inelastically scattered from an even-even nucleus ($A\sim30$). The levels excited are odd-spin odd-parity states with spin changes as shown. Relative intensities are shown by σ_T.

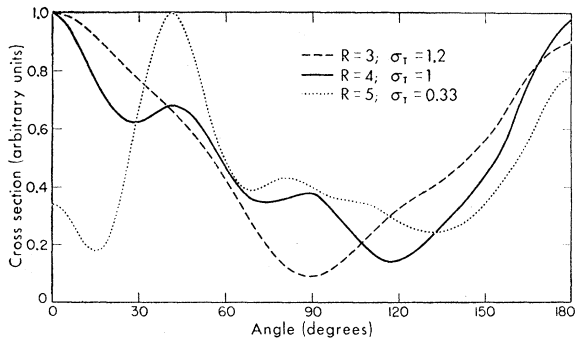

FIG. 7. Angular distribution of 15-Mev neutrons inelastically scattered from an even-even nucleus ($A\sim30$). Curves show the effect of changing the radius of the distorting potential. Changing the depth of the distorting potential produces similar changes. Relative cross-sections are indicated by σ_T. The spin change is $0+\rightarrow 2+$.

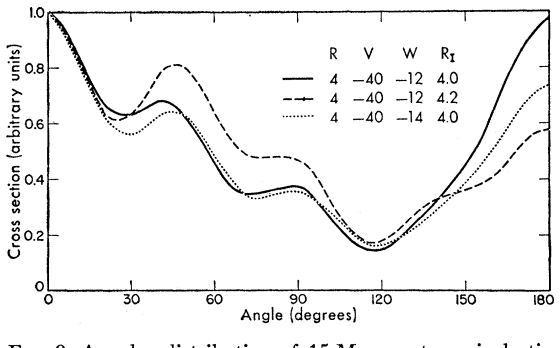

FIG. 9. Angular distribution of 15-Mev neutrons inelastically scattered from an even-even nucleus ($A\sim30$), with excitation of 2+ states. The curves illustrate the effect of changing the imaginary part of the distorting potential W and the interaction radius R_I. The radius of the distorting potential is R, and its real well depth V. Energies are quoted in Mev, and lengths in units of 10^{-13} cm.

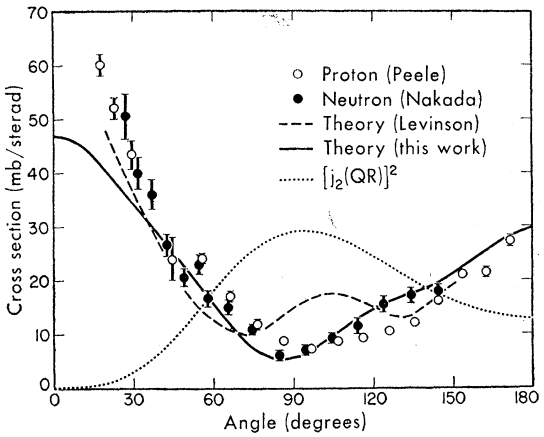

FIG. 10. Angular distribution of 14-Mev nucleons inelastically scattered from the 2+ level at 4.43 Mev in C^{12}. The curves compare the theory of this work and the theory of Levinson and Banerjee with the experimental data. The optical-model parameters used in our calculation are listed in Table III.

et al.[22] was used for guidance in the choice of optical-model parameters.

3. Inelastic Scattering of Protons and Neutrons from Carbon

There are more experimental data[30,31] available on the inelastic scattering of protons from the 4.43-Mev level in C^{12} than for any other level. There exist 14-Mev neutron data also.[32]

An attempt has been made to fit the data at 14, 19.4, and 39.6 Mev (lab).

The excited state is assumed to be formed from the ground state by raising a particle from the $p_{\frac{3}{2}}$ shell to the $p_{\frac{1}{2}}$ shell.

In Fig. 10 the 14-Mev neutron and proton data and the theoretical curve calculated by Levinson and Banerjee[5] are compared with a calculation using the theory developed in this work. The neutron and proton data are very similar; the minimum in the proton data near 90° is shifted toward larger angles by about 10°, as one would expect due to the Coulomb repulsions.[33] Because the Coulomb distortion was not included in our work, our curve should agree more closely with the neutron data. The theory predicts a lower cross section at angles less than 40° than is actually observed; for larger angles, however, the agreement is quite satisfactory.

It must be stressed that both our theory and that of Levinson and Banerjee had to be renormalized. Our calculation had to be multiplied by the number 220 to get the result shown in Fig. 10. However, the calculation was carried out with the length parameter γ set equal to unity [Eq. (2)]. If instead one sets γ equal to the force range, and recalls from Sec. V that use of a square well rather than a rounded well reduces the absolute magnitude of the cross section by a factor of 5 to 6, the discrepancy between calculated and measured cross sections is reduced to a factor of about 14. Because of the uncertainty in the factors just mentioned this must be regarded as essentially in agreement with the factor ~ 6 by which Levinson and Banerjee renormalized their theory.

Figure 11 compares our theory with the experimental proton data at 19.4 Mev (lab). The agreement is only qualitative, and is not as satisfactory as the fit obtained by Levinson and Banerjee.

Figure 12 shows the experimental data for scattering of 39.6-Mev protons. The theoretical curve agrees only qualitatively, exhibiting much larger oscillations than indicated by experiment. It is interesting to note, however, that there is evidence for alternate maxima and minima at 90°, 110°, 140°, and ~180°, which are predicted by the theory. The size of the oscillations would probably be reduced by allowing the direct interaction to occur throughout a region of finite thickness near the nuclear surface.

In Table III we summarize the parameters used in the calculation of the inelastic scattering from carbon. The imaginary part W of the distorting potential shows the correct dependence on the bombarding energy. The calculation at 39.6 Mev does not represent a very thorough search for a best fit, and the parameters R

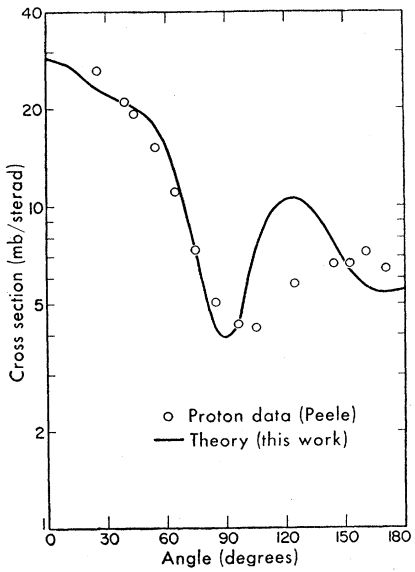

FIG. 11. Angular distribution of 19.4-Mev protons inelastically scattered from the 2+ level at 4.43 Mev in C^{12}. The optical-model parameters are listed in Table III.

[30] R. W. Peele, Phys. Rev. **105**, 1311 (1957).
[31] S. Chen and N. M. Hintz, University of Minnesota Progress Report, March, 1958 (unpublished).
[32] Anderson, Gardner, McClure, Nakada, and Wong, Phys. Rev. **111**, 572 (1958).
[33] According to classical mechanics, a 14-Mev proton with impact parameter equal to the C^{12} radius would be scattered by that nucleus through an angle of about 12°. The agreement between the experimental shift of the minimum in the proton and neutron angular distributions and this prediction tends to confirm our assumption of a surface interaction.

and V might quite possibly be chosen differently, and in better agreement with our expectations.

In summary we may say that a rather good agreement of theory with experiment was obtained for 14-Mev neutron scattering, but only qualitative agreement was obtained with the two higher-energy proton experiments. Even the qualitative agreement is, however, a marked improvement over the plane-wave Born approximation which predicts distributions similar to the one shown in Fig. 5 with very small forward scattering.

4. Proton Inelastic Scattering from Oxygen

Hornyak and Sherr[34] have measured the angular distribution of 19-Mev protons inelastically scattered from a number of states in O^{16}. The most strongly excited state is the level at 6.14 Mev. Its spin and parity are known to be 3−. However, to illustrate that the theory adequately distinguishes this from the assumption that the level in question has spin and parity 1−, two theoretical curves corresponding to these assumptions, together with the experimental results are shown in Fig. 13. For the theoretical curve designated 3−, the single-particle transition $1p_{\frac{1}{2}} \rightarrow 1d_{\frac{5}{2}}$ was assumed.

The maxima and minima are predicted by the 3− curve to within about 15° of the observed values. The cross section in the backward hemisphere is too large compared with the forward-hemisphere scattering. Since volume interactions tend to reduce this ratio, the agreement could probably be improved by taking these interactions into account. Nevertheless the agreement of theory with experiment is fair, and represents a vast improvement over the simple plane-wave Born approximation.

Just as for carbon, the calculated cross section (for 3−) has been renormalized, this time by a factor of 210. Again if we set the length parameter equal to the force range, and recall that use of a square rather than a round distorting potential can reduce the absolute magnitude of the cross section by a factor of 5 or 6, the remaining discrepancy is a factor of ∼10.

The square-well parameters used in the above calculation were

$$V_D = -(40+16i)\ \text{Mev}, \quad \text{for } r<3.35\times10^{-13}\ \text{cm}$$
$$=0, \quad \text{otherwise},$$

and the interaction radius used was 3.6×10^{-13} cm.

TABLE III. Summary of parameters used in analysis of inelastic scattering from the 4.43-Mev level of C^{12}.

Projectile	Energy (lab system) (Mev)	R_I (10^{-13} cm)	R (10^{-13} cm)	V (Mev)	W (Mev)	F[a]
			This calculation			
neutron	14	3.45	3.2	35	10	∼14
proton	19.4	3.3	2.98	35	14	∼9
proton	39.6	3.5	3.2	35	20	∼7 −0.7
			Levinson-Banerjee			
proton	14	···	2.98	∼39.4	···	∼6
proton	19.4	···	2.98	34.4	8	∼6

[a] Normalizing factor by which theory must be multiplied to obtain agreement with experiment.

[34] W. F. Hornyak and R. Sherr, Phys. Rev. **100**, 1409 (1955).

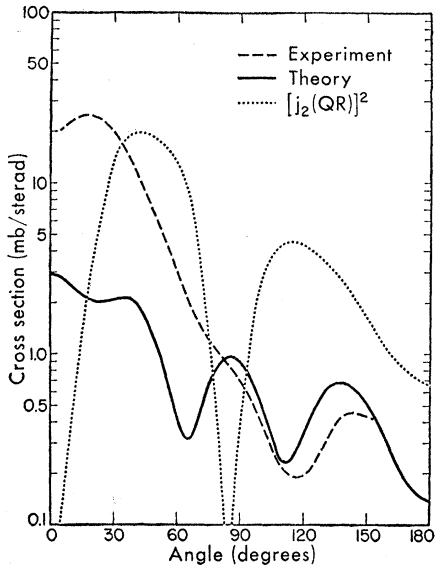

FIG. 12. Angular distribution of 39.6-Mev protons inelastically scattered from the 2+ level at 4.43 Mev in C^{12}. The optical-model parameters are listed in Table III.

5. Inelastic Scattering of Alpha Particles by Carbon

Watters[29] has measured the inelastic scattering of 31.5-Mev alpha particles from the 4.43-Mev level in C^{12}. He shows that the simple plane-wave Born approximation gives a reasonable fit to the data. The minima of the plane-wave approximation are actually zero, which does not agree with experiment. One might

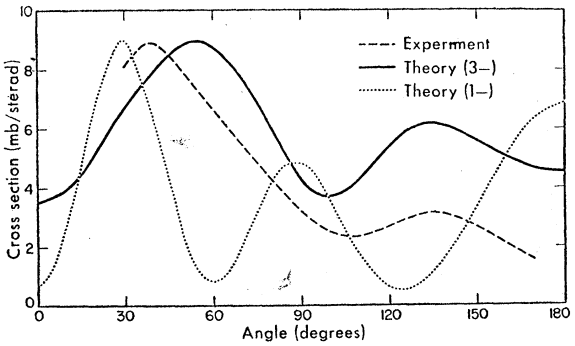

FIG. 13. Angular distribution of 19-Mev protons inelastically scattered from the 3− level at 6.14 Mev in O^{16}. The experimental curve is a smooth curve drawn through the results of Sherr and Hornyak. The calculation labeled (1−) corresponds to assuming the excited state has this spin and parity, and is included to illustrate that the theory can discriminate between various assumptions concerning the spin and parity of the excited state. The optical-model parameters are listed in the text.

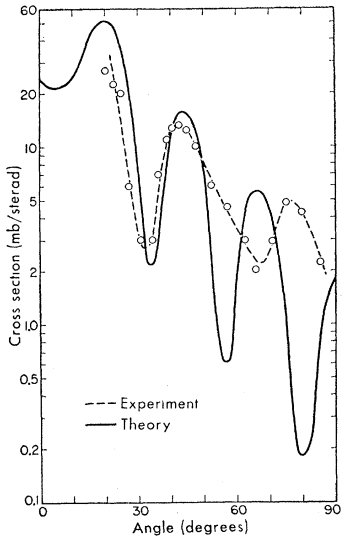

FIG. 14. Angular distribution of 31.5-Mev alpha particles inelastically scattered from the 2+ level at 4.43 Mev in C^{12}. The optical-model parameters are listed in the text.

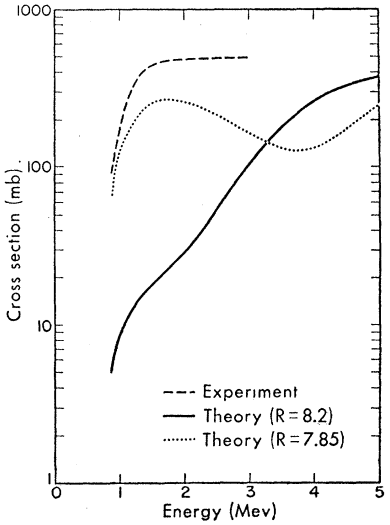

FIG. 15. Neutron-excitation function for the 2+ level at 0.803 Mev in Pb^{206}. The theoretical curves correspond to inelastic scattering by direct interaction at the nuclear surface. The experimental curve is deduced from the work of Day and Lind. The optical-model parameters are $V=-40$ Mev, $W=-2.4$ Mev, and the radii in units of 10^{-13} cm are indicated in the figure. The theory was multiplied by a factor of 10 (see text).

expect the zeros to be removed by the introduction of a distorting potential. Several calculations have been made in an attempt to fit the data with our theory, and such a calculation is shown in Fig. 14. The theory gives too large a ratio of maxima to minima, but this might be removed by a more extensive search for a fit. The first two peaks are in agreement with experiment. At larger angles, however, the experimental positions of peaks and valleys are shifted toward larger angles. This could be accounted for by Coulomb repulsion (not included in the present theory) which would be more effective for large-angle scattering.

The optical-model parameters used for the curve shown in Fig. 14 are

$$V_D=-(20+14i)\text{ Mev},\quad \text{for}\quad r<3.1\times10^{-13}\text{ cm}$$
$$=0,\quad \text{otherwise},$$

and the interaction radius used was $R_I=5.5\times10^{-13}$ cm.

It is not clear what depth one should adopt for the direct-interaction potential. When the same value is used as that quoted for nucleon scattering, the calculated cross section is smaller by a factor of ~2.7 than the experimental result. Of course some of this discrepancy may be due to use of a square well. For square wells with a depth of 35 to 40 Mev, we have seen that the absolute magnitude of the cross section is less by about a factor of 5.5 than for a corresponding calculation using a rounded potential. For our calculation we used a real square-well depth of 20 Mev, so that it is no longer clear what this correction factor would be.

The Bessel-function angular distribution predicted by the plane-wave Born approximation fits the alpha-particle scattering by both carbon and magnesium quite well,[29] in contrast to the poor fit given by that approximation to nucleon scattering by carbon and oxygen.

6. Excitation Function for Inelastic Scattering of Neutrons by Lead

The cross section for inelastic scattering of neutrons from the 0.803-Mev level in Pb^{206} has been measured by Day and Lind[35] for incident energies up to 3 Mev. The excitation function deduced from their data is shown in Fig. 15. Also shown are calculations for the excitation of this level, assuming a direct interaction mechanism. As was pointed out in Sec. V, this level is strongly admixed, and the $(p_{\frac{1}{2}}p_{\frac{3}{2}})^{-1}$ component of the level at 0.803 Mev is excited with an intensity ~100 times as great as the $(p_{\frac{1}{2}}f_{\frac{5}{2}})^{-1}$ component. The curves shown represent the cross section for excitation of a pure $(p_{\frac{1}{2}}p_{\frac{3}{2}})^{-1}$ level.

The calculated curves are less than $\frac{1}{10}$ of the experimental cross section. However, recalling that the theory ought to be renormalized as has already been discussed, we see it is possible that the direct interactions may contribute significantly to excitation of this level, even at these low energies.

It is probable that compound-nucleus formation and decay is the dominant mechanism at energies near threshold. However, in Pb^{206} there are about 20 excited states between 1.3 and 3.5 Mev, so that competition in the decay of the compound nucleus amongst these states may rapidly damp the compound-nucleus contribution. The experimental cross section, nevertheless, shows no sign of decreasing between 2 and 3 Mev, indicating that the direct excitation may already be making an important contribution to the excitation of the 0.803-Mev level. The answer to these speculations

[35] David Lind and R. Day (private communication).

probably lies in the measurement of the angular distribution. A simple calculation of the angular distribution indicates that the forward-to-backward scattering ratio may be quite large.

7. Concluding Remarks

For inelastic nucleon scattering by complex nuclei of more than a few Mev incident energy, a direct-interaction mechanism is the predominant mode of excitation of the low-lying nuclear levels, particularly those whose overlap with the ground state is large. Inelastic scattering should therefore provide an important means of studying these highly excited levels, because, as for stripping reactions, the scattering depends on the nature of the ground and excited states more intimately than it does for scattering through a compound-nucleus channel. That a few of the levels are excited much more strongly than others by the direct interaction inelastic scattering is important from the experimentalist's point of view, because it means that the resolution of scattering events from various levels in the target nucleus can more readily be achieved. The experimental work by Cohen and co-workers on Pb^{206} indicates that only a few states are strongly excited.[36–38] Tamura and Choudhury have met with some success in analyzing these experiments, using the plane-wave Born-approximation model of direct interactions.[39]

We have compared the theory of direct interactions developed in this work with some of the more appropriate experimental measurements. It appears that within the range of validity of the theory, sufficiently good agreement can be obtained to permit one to deduce information on the spins and parities of excited states when the ground-state spin and parity are known. The analysis would be particularly unambiguous if the optical-model parameters could be fixed by fitting the theory to the angular distribution from an excited state of known spin and parity.

The modest success of our surface-interaction model demonstrates the usually dominant role of the distorting potential in determining angular distributions. The extent to which the surface-interaction model is successful measures the degree to which the cross section is independent of the single-particle configurations involved, aside from their importance in determining the absolute cross sections (see Sec. IV-4). Nevertheless, direct interactions will undoubtedly provide an important means of studying nuclear energy levels, and may contribute to our understanding of the physical significance of the optical model. In this connection, Levinson and Banerjee[5] found that the optical-model parameters that fit the elastic-scattering data are not the ones that give the best fit to the inelastic data. Indeed, in our calculations, the real part of the distorting well depth was always smaller than indicated by the elastic-scattering analysis. In particular, the parameters used by Beyster *et al.*[22] to fit the elastic scattering of 14-Mev neutrons by the 4.43-Mev level in carbon were used by us to calculate the cross section for the inelastic scattering, and the theoretical curve bore little resemblance to the experimental curve. It is not clear, therefore, from these analyses that the optical-model parameters for elastic scattering should be the same as for mechanisms that contribute to the absorption from the incident beam.

ACKNOWLEDGMENTS

The author would like to express his appreciation to Professor K. W. Ford for many helpful discussions throughout the course of this work.

A grant from the Physics Department, Indiana University, and National Science Foundation is gratefully acknowledged, as is the hospitality of Los Alamos Scientific Laboratory, where this work was carried out.

APPENDIX

The cross section for direct-interaction inelastic scattering can be simply written for the four cases: 1. One extra-core nucleon, 2. Closed shell nucleus, 3. Two extra-core nucleons, and 4. Two holes in closed shell.

Define the differential cross section.

$$\sigma_L(\theta)=\frac{k'}{k}\left(\frac{2m}{\hbar^2}\right)^2\frac{1}{2j+1}Z^2(ljl'j';\tfrac{1}{2}L)\sum_{pp'qq'n}i^{p-p'+q-q'}$$
$$\times\{(2p'+1)(2q'+1)\}^{\frac{1}{2}}(2p+1)(2q+1)$$
$$\times C(pLp';000)C(qLq';000)C(pqn;000)$$
$$\times C(p'q'n;000)R_{p'Lp}R^*_{q'Lq}$$
$$\times W(pp'qq';Ln)P_n(\cos\theta),$$

and total cross section

$$\sigma_L=4\pi\frac{k'}{k}\left(\frac{2m}{\hbar^2}\right)^2\frac{1}{2j+1}Z^2(ljl'j';\tfrac{1}{2}L)$$
$$\times\sum_{pp'}(2p+1)C^2(pLp';000)|R_{p'Lp}|^2.$$

Then for the four cases listed above

$$\sigma_1=\textstyle\sum_L\sigma_L,$$
$$\sigma_2=(2j+1)\sigma_J,$$
$$\sigma_3=2\sigma_J,$$
$$\sigma_4=(2j-1)^2|\textstyle\sum_\alpha(J[\![\alpha j)(aj]\!]0)|^2\sigma_J,$$

where in the last three cases the ground-state spin is zero, and the excited state spin is J. The symbol $(\alpha I]\!]J)$ is a coefficient of fractional parentage

$$(\alpha I]\!]J)\equiv(j^{N-3}(\alpha I)J]\!]j^{N-2}J),$$

where $N=2j+1$.

[36] B. L. Cohen, Phys. Rev. **105**, 1549 (1957).
[37] B. L. Cohen and S. W. Mosko, Phys. Rev. **106**, 995 (1957).
[38] B. L. Cohen and A. G. Rubin, Phys. Rev. **111**, 1568 (1958).
[39] T. Tamura and D. C. Choudhury, Phys. Rev. **113**, 552 (1959).